JMEPEG (1996) 5:615-620

Study of Aging and Embrittlement of Microalloyed Steel Bars

B. Campillo, R. Perez, and L. Martinez

The aging of hooks, anchors, and other bent reinforcing steel bars in concrete structures are considered in modern international standards. Rebend test procedures have been designed in order to predict the aging embrittlement susceptibility by submerging bent reinforcing bar specimens in boiling water. Subsequently the bars are rebent or straightened in order to determine the loss of ductility or embrittlement of the aged material. The present work considers the influence of carbon, sulfur, and niobium on the performance of reinforcing bars in rebend tests of 300 heats of microalloyed steel bars with a variety of compositions. The microstructural evidence and the statistical results clearly indicate the strong influence of carbon and sulfur on rebend failure, while niobium-rich precipitates contribute to the hardening of the ferrite grains during aging.

Keywords
aging, microalloyed, rebend, reinforced steel

1. Introduction

THE DEVELOPMENTof high-strength, low-alloy (HSLA) steel reinforcing bars as substitutes for medium-carbon steel bars is one of the main trends in the steel industry. The required properties of reinforcing bar steels are given in various specifications. Besides the requirements for a certain amount of yield and ultimate tensile strength, and elongation to fracture, properties with respect to safety and workability are of increasing importance. A bend test is usually required to predict the performance of reinforcing bars under working conditions in the field. A rebend test procedure has been introduced to consider the possible embrittlement of bent bars after a few years of service (Ref 1). The rebend test is performed in three steps: (1) the bar is bent; (2) the bar is aged by being submerged in boiling water; and (3) the bar is bent back straight. Depending on certain characteristics of the steel microstructure, the bar may fail by brittle fracture in step 3. In this case, the batch that this bar represents is rejected.

Plastic deformation and temperature develop important microstructural transformations in materials. The effects of carbon, sulfur, and niobium on the behavior characteristics of different types of steels have been widely studied at high temperature. Thus, for example, in low-carbon steels it has been found that the ductility loss in high-strain-rate deformation is caused by the dynamic precipitation of iron-rich (Fe-Mn)S particles within the γ grains and γ grain boundaries, and that ductility loss is increased by increasing the sulfur content (Ref 2). On the other hand, the ductility loss in low-strain-rate deformation is caused by the dynamic precipitation of Nb(C,N) particles. This ductility loss is greatly reduced by decreasing the sulfur content to less than 10 ppm (Ref 2).

B. Campillo, Facultad de Quimica, Universidad Nacional Autonoma de Mexico, Ciudad Universitaria, Mexico D.F.; and **R. Perez** and **L. Martinez,** Instituto de Fisica, Universidad Nacional Autonoma de Mexico, P.O. Box 139B, 62191 Cuernavaca, Morelos, Mexico.

Niobium and sulfur are also detrimental to the hot ductility of as-cast C-Mn-Al steels (Ref 3). Reduction of niobium and sulfur content will improve ductility and reduce transverse cracking. In general, the addition of niobium results in the presence of a fine uniform precipitation of Nb(C,N) particles. However, the addition of sulfur results in the precipitation of sulfides at the grain boundaries and also in a fine precipitation of iron oxysulfides, similar in size and distribution to the Nb(C,N) precipitates (Ref 3).

In niobium HSLA steels, the strain-induced precipitation of Nb(C,N) leads to strengthening of austenite, with a maximum occurring when particles are 2 to 3 nm in size, independent of steel composition or prior reheating/roughing conditions (Ref 4). The maximum strengthening occurs at an early stage, estimated to be between 5 to 15% of equilibrium precipitation. The strengthening increment then decays rapidly, because the number of particles per unit volume decreases as particle size increases (Ref 4). The mechanisms leading to the effects of reheating and roughing conditions on the subsequent strain deformation precipitation after a finished deformation are not clear, but a temperature-dependent clustering of niobium and carbon atoms provides a consistent explanation of the observations (Ref 4).

In low-carbon, high-manganese steels after hot rolling, no intergranular niobium carbonitride precipitation in austenite was found in the absence of plastic deformation. The amount of Nb(C,N) precipitation in austenite was strongly influenced by rolling conditions (Ref 5). The Nb(C,N) particle sizes in austenite increase with niobium content. Also, no interphase or ferrite precipitation of niobium carbonitrides was observed in any of the higher-manganese steels, which transformed to an acicular ferrite microstructure on air cooling (Ref 5).

In low-carbon, low-alloy steels, the hot cracking of the continuous casting slab surface can be explained in terms of carbide and/or nitride precipitation behavior (Ref 6). The origin of hot cracking during the direct rolling process also lies in the precipitation of carbides and/or nitrides and is not related to the severe embrittlement caused by a similar mechanism with dynamic precipitation of sulfides, which is usually observed in high-strain-rate deformation after reheating at higher temperatures.

Little attention has been given in the literature to the influence of carbon, sulfur, and niobium in microalloyed steels that have been through bending and rebending processes and subsequently aged at temperatures of boiling water. The present work is based on investigation of the effects of these common steel constituents on some of the mechanical properties of microalloyed steel bars when they have been through bending and rebending test procedures.

2. Experiment

The steels for reinforcing bars considered in this work were fabricated employing the standard blast furnace/basic oxygen furnace/ladle furnace sequence. The pig iron produced in the blast furnace was combined with 20% steel scrap in the basic oxygen furnace. The alloy composition of the steel was adjusted in the ladle furnace, where a nitrogen jet was employed to agitate the melt and homogenize the alloying elements. The melts were continuously cast to form billets 125 mm per side square section and 8 m long, then were air cooled. The billets were reheated at 1150 °C for 2 h and hot rolled to produce 40 mm nominal diameter deformed reinforcing bars. The temperature at the end of the finishing section of the rolling process was 1050 °C.

The alloy composition of the steel microalloyed with niobium and the thermomechanical process were designed in order to obtain mechanical properties appropriate to comply with the BS 4449 standard (Ref 1) of nonweldable grade. In the present work, 300 heats of 120 tons each were considered. The range of alloy chemical compositions (wt%) was 0.24 to 0.43 C, 1.30 to 1.42 Mn, 0.0035 max P, 0.004 to 0.007 S, 0.18 to 0.23

Table 1 Chemical compositions of the steels studied

Steel No.	Composition, wt %								Rebend test failure
	C	Si	P	S	Mn	Nb	Al	N	
1	0.26	0.21	0.017	0.032	1.35	0.044	0.004	0.008	X
2	0.31	0.24	0.022	0.017	1.42	0.030	0.004	0.007	
3	0.34	0.17	0.019	0.034	1.38	0.034	0.006	0.005	
4	0.37	0.21	0.014	0.039	1.32	0.043	0.004	0.007	X
5	0.43	0.22	0.016	0.030	1.37	0.040	0.003	0.007	
6	0.46	0.19	0.010	0.024	1.38	0.046	0.005	0.009	

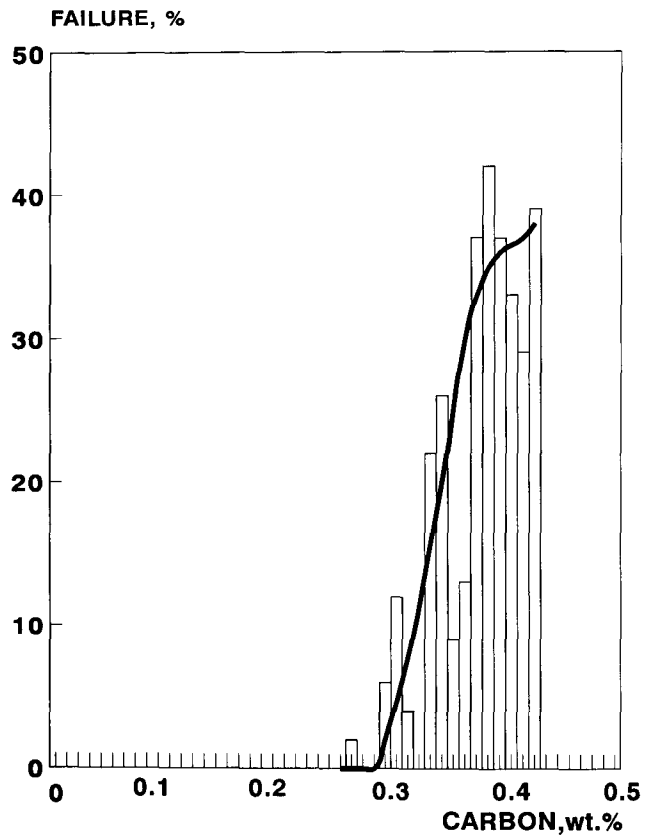

Fig. 1 Effect of carbon content on the failure frequency during the rebend test

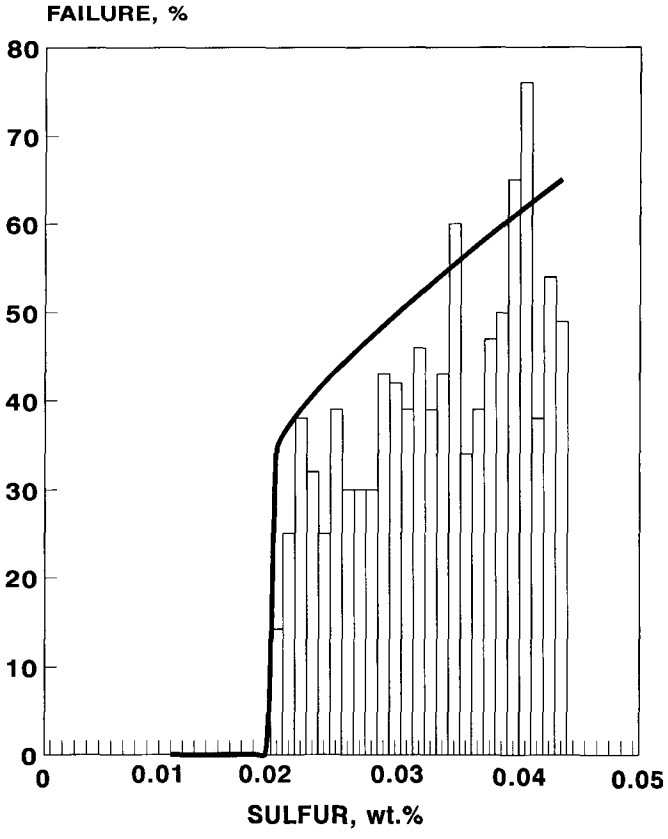

Fig. 2 Effect of sulfur content on the failure frequency during the rebend test

Si, 0.028 to 0.046 Nb, 0.005 to 0.010 N, and 0.003 to 0.007 Al. From the 300 heats, six representative samples were selected for detailed experimental study. The chemical composition of these six samples is presented in Table 1.

BS 4449 requires yield strength above a minimum of 460 MPa and elongation to fracture above 12%. These tests were performed in a standard universal testing machine of 200 metric tons capacity. A bend machine was also employed to perform 180° tests on 1.2 m length samples using a mandrel 120 mm in diameter. The rebend tests were designed to simulate the role of aging on the embrittlement of bend sections of the bars during construction. The bending procedure was introduced into the bending machine to make a 45° bend using a 200 mm diameter mandrel. The sample was subsequently submerged in boiling water for 60 min to age. Finally, the sample was introduced into the bending machine in a reverse mode in an attempt to make the bar straight. If the sample did not fracture by this procedure, the rebend test was passed.

Metallographic characterization of the six samples was carried out. Particular attention was given to samples 1, 4, and 5 of Table 1, which failed during the rebend test. The specimen were sliced along the bar axis in the central part near the fractured surface, then ground with sand paper, polished in alumina powder, and finally etched with Nital 2. The observations were carried out in a scanning electron microscope with electron dispersive analysis by x-ray (EDX).

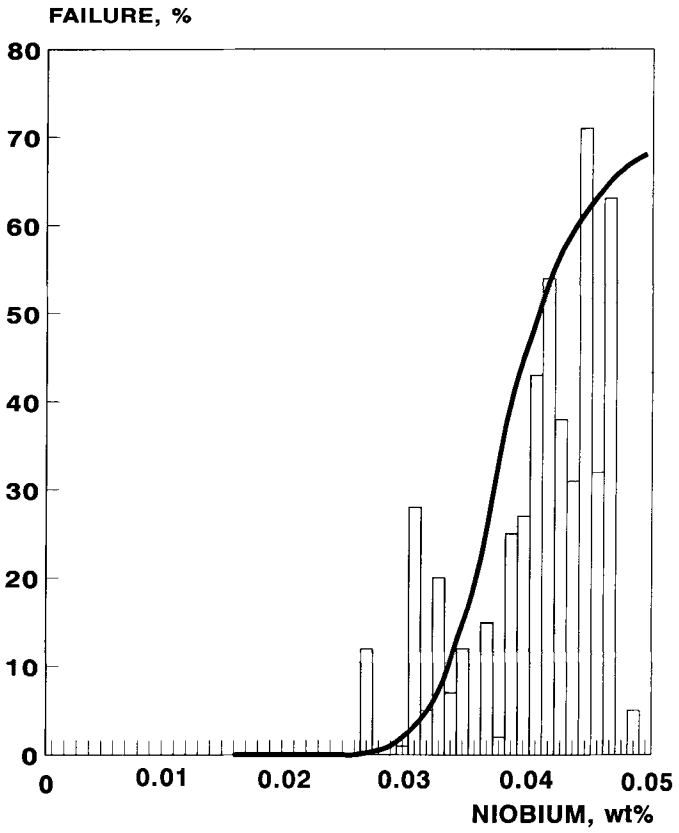

Fig. 3 Effect of niobium content on the failure frequency during the rebend test

Samples of the unbent material of the six alloys shown in Table 1 were employed for a test procedure to detect hardening by aging. Eight cylinders obtained from the core of each bar were machined to dimensions of 12 mm diameter and 15 mm height. The samples were annealed at 940 °C for 1 h, slowly cooled (0.035 °C/s) between 780 and 500 °C, and finally air cooled. The decarburized layer of the cylinders was ground off. Three cylinders of each set were deformed in compression by 10%, and the other three were compressed 50% with an Instron machine. Some of the samples were subsequently subjected to aging treatments of 30 and 60 min in boiling water. The specimens of each group (deformed 10% or 50%, aged 30 or 60 min) were polished and etched employing alumina or Nital 2, respectively, in order to develop the ferrite and pearlite grains of the microstructure. Microhardness Vickers indents were performed in the ferrite and pearlite grains using a 10 g load in a Matsuzawa microindenter. Ten measurements in different grains were performed to obtain an average value. Micrographs of specimens from selected steel bars that failed during the rebend tests were obtained with a JEOL-T-200 SEM machine with an EDX analyzer.

3. Results and Discussion

It has been found that carbon, sulfur, and niobium have a notorious correlation with rebend failure. Other elements, such as manganese, silicon, and phosphorus, are not correlated with rebend failures.

Figures 1 to 3 show the results of the rebend tests, where the failure frequency is plotted against the weight percent of the respective amount. Figure 1 shows that at higher carbon contents, the frequency of rebend failure increases strongly. Figure 2 shows the effect of sulfur on the failure frequency, where similar behavior as in the carbon case is obtained. Increasing the sulfur content induces the formation of sulfide compounds such as manganese sulfide, which causes anisotropy of ductility relative to rolling directions (Ref 7, 8). Figure 3 represents the effect of niobium on the failure frequency. The same trend as in the sulfur and carbon cases is obtained: increasing the niobium content also increases the frequency of failure.

Some of the microstructural characteristics of these microalloyed steel bars are presented in Fig. 4 to 6. Figure 4 shows a section of one of the specimens that failed during the rebend test. The elongated light gray inclusions have been identified by EDX as manganese sulfides. The dark inclusions are related to aluminum oxides or spinel phases (Ref 9). The sulfide inclusion ends in a surface fracture, suggesting that cracking could be related to the presence of these kinds of inclusions (Ref 10). Crack initiation at sulfur manganese compounds has been widely reported (Ref 11, 12). Figure 5 shows another morphological aspect of manganese sulfide inclusions. In Fig. 4 and 5 there is clear evidence of cavities in the interphase regions between the matrix and the manganese sulfide precipitates. Figure 6, on the other hand, shows evidence of pearlite tearing, which has also been observed in bent bar specimens (Ref 13). These observations indicate that the role of carbon and sulfur in the rebend failure of bent bars may be due to the formation of microcracks in the interphase regions (ferrite/manganese sulfide) or in the pearlite grains (Ref 14). If the bar reaches step 3

of the rebend test in a severely microcracked condition, failure will occur.

The role of niobium was found to correlate with the aging stage of the rebend test. Vickers hardness measurements were carried out on samples of the same steels to study the behavior and response to a deformation aging process. Figure 7 shows the response of the ferrite phase after being deformed and aged. There are clear increases of hardness after deformation due to the strain-hardening process, and there are also clear signs of an age-hardening effect. It is important to point out the recent reports on the importance of precipitation of carbides, nitrides, or carbonitrides in inducing strain aging effects (Ref 15). Figure 8, on the other hand, shows the response of the pearlite grains after being deformed and aged. In this figure, there are also signs of increased microhardness due to strain hardness effects. However, there is no pronounced association between the effects on this mechanical property and the amount of plastic deformation. Some of these results have been related to the pinning of dislocation by carbide compounds (Ref 7, 16).

The effect of niobium on the microhardness of the ferrite phase is shown in Fig. 9. The two deformation values (10 and 50%) are included in this graph. Increasing the niobium content gives rise to an increase in microhardness, which is usually related to a precipitation-hardening effect (Ref 16). Observations of deformed (50%) and deformed and aged material are shown in Fig. 10(a) and (b), respectively. In Fig. 10(a), a high dislocation density is due to the 50% deformation, and several relatively large niobium-rich precipitates are present (Ref 17). In Fig. 10(b), after aging, the field of dislocations has been reduced and many small precipitates are formed. It is conceivable that the contribution of niobium to the reported increase in the frequency of rebend failure can be associated with the enhancement of the propagation of pre-existing cracks or cavities through the hardened ferrite grains. The lowering of the carbon content of the steel below 0.25 wt% and the sulfur content below 0.018 wt% significantly reduce microcrack formation. The frequency of failure is reduced below 0%, regardless of the niobium content, in the range of compositions studied here.

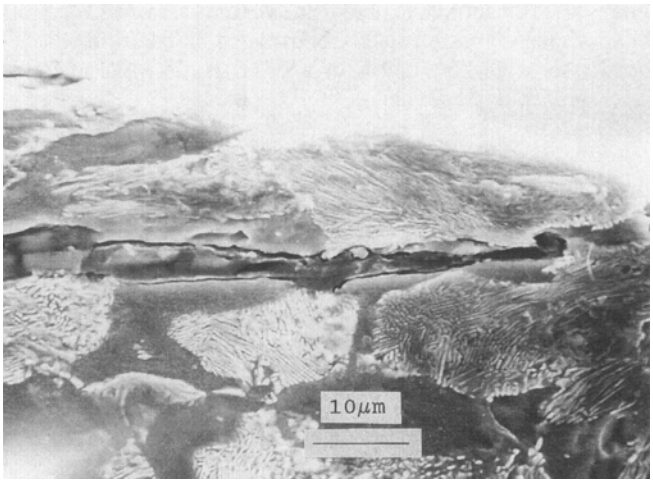

Fig. 4 SEM image of a longitudinal cross section of sample 1 of Table 1, showing light gray inclusions (manganese sulfides) connected with the fracture surface of the bar after failure during the rebend test

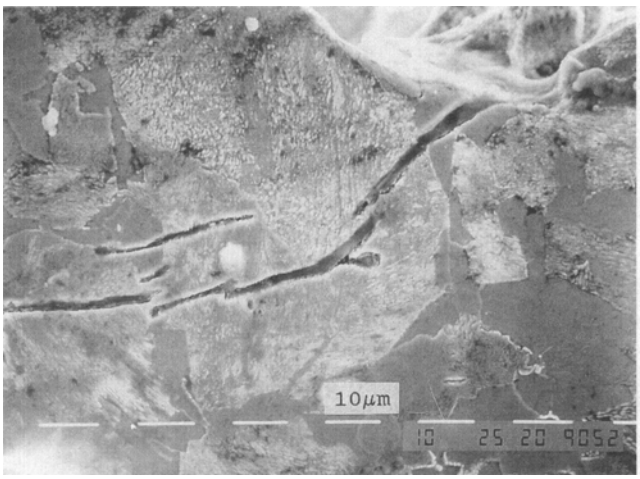

Fig. 5 SEM image of the cross section of sample 4 of Table 1, showing the inclusion running beneath the fracture surface where some localized voids or separations occurred after the steel failed during the rebend test

4. Conclusions

Rebend failures were found to be statistically associated to higher levels of carbon, sulfur, and niobium of the microalloyed steels reported here. Microstructural examination revealed that in the carbon-rich phase of the steel, the pearlite, microcracks are formed by pearlite tearing. In the microstructure near the fractured specimens, cracks tended to form in the metal/manganese sulfide interface. It can be concluded that the contribution of carbon and sulfur to the rebend failure is due to microcrack formation in the 45° bend part of the rebend test. Niobium appears to contribute in the aging stage of the test. During aging the ferrite grains exhibited considerable hardening. At the final stage of the test, the high-carbon, -sulfur, and -niobium steel bars were very susceptible to failure.

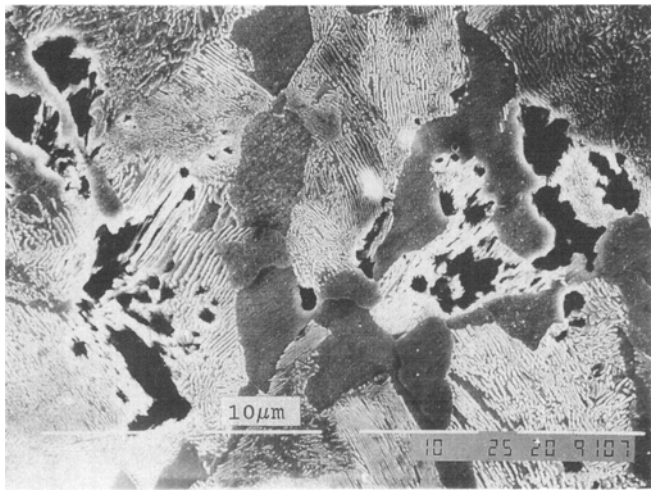

Fig. 6 SEM image of a cross section that shows regions where pearlite tearing is present

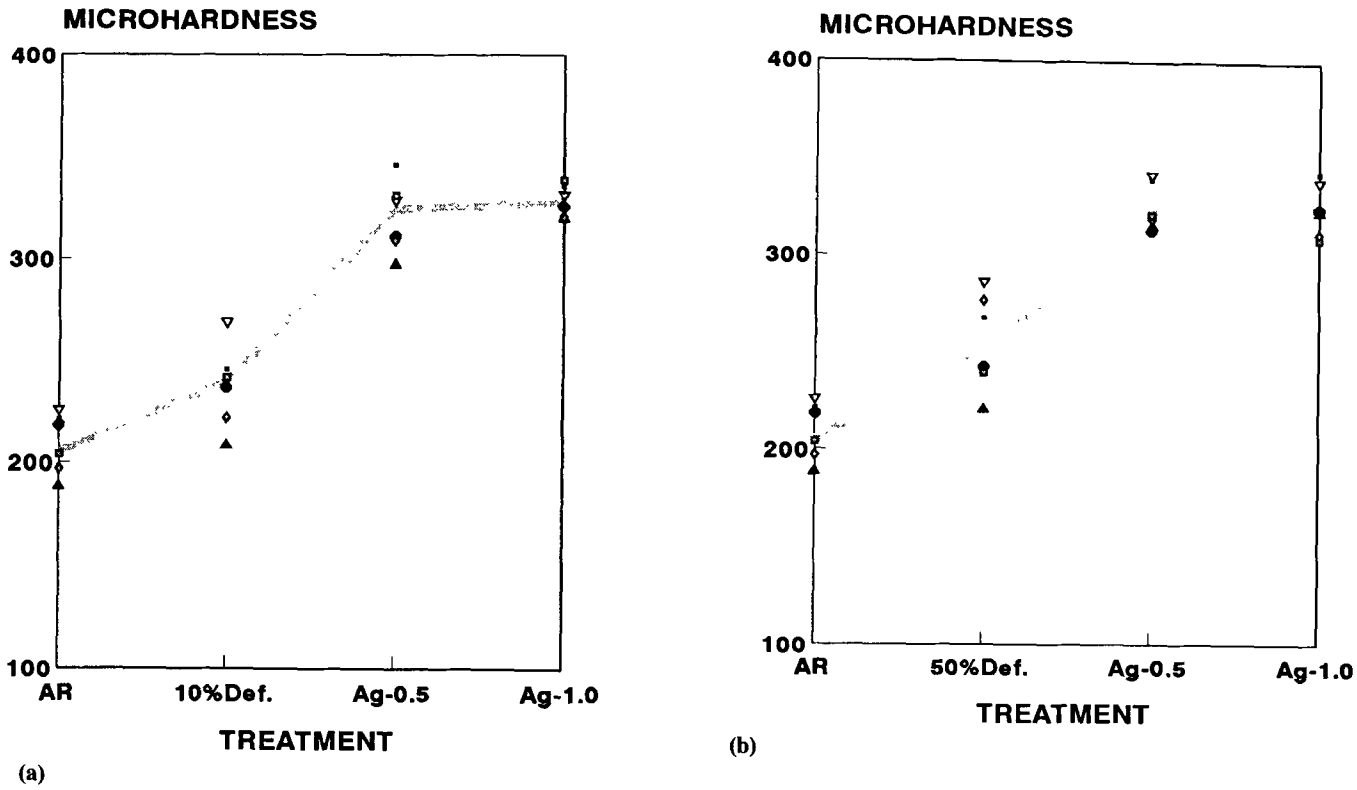

Fig. 7 Microhardness changes in the ferrite phase as a function of the aging treatment process after (a) 10% and (b) 50% cold deformation. Sample 1 of Table 1 is represented by the squares, sample 2 by the rhombuses, sample 3 by the triangles, sample 4 by the circles, sample 5 by the inverted triangles, and sample 6 by the plus signs.

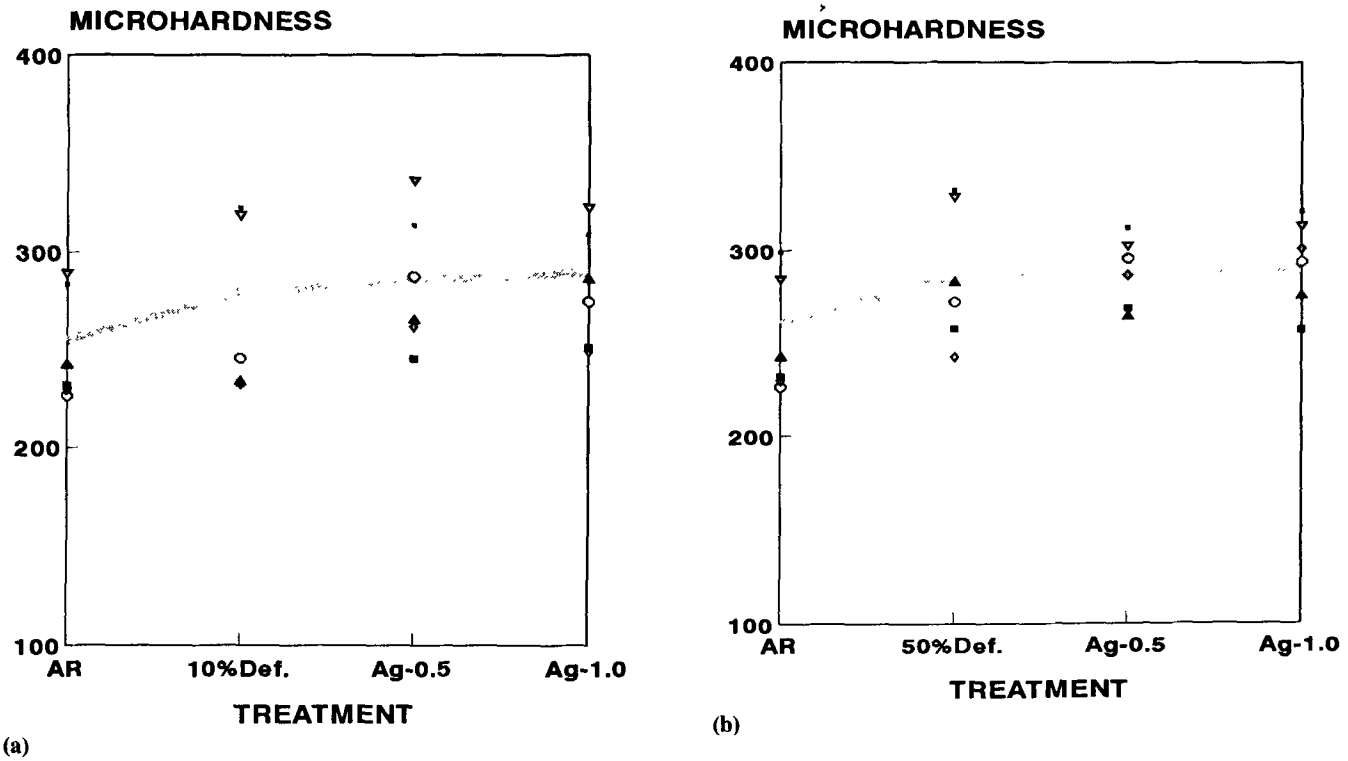

Fig. 8 Microhardness changes in the pearlite phase as a function of the treatment process after (a) 10% and (b) 50% cold deformation. Sample 1 of Table 1 is represented by the squares, sample 2 by the rhombuses, sample 3 by the triangles, sample 4 by the circles, sample 5 by the inverted triangles, and sample 6 by the plus signs.

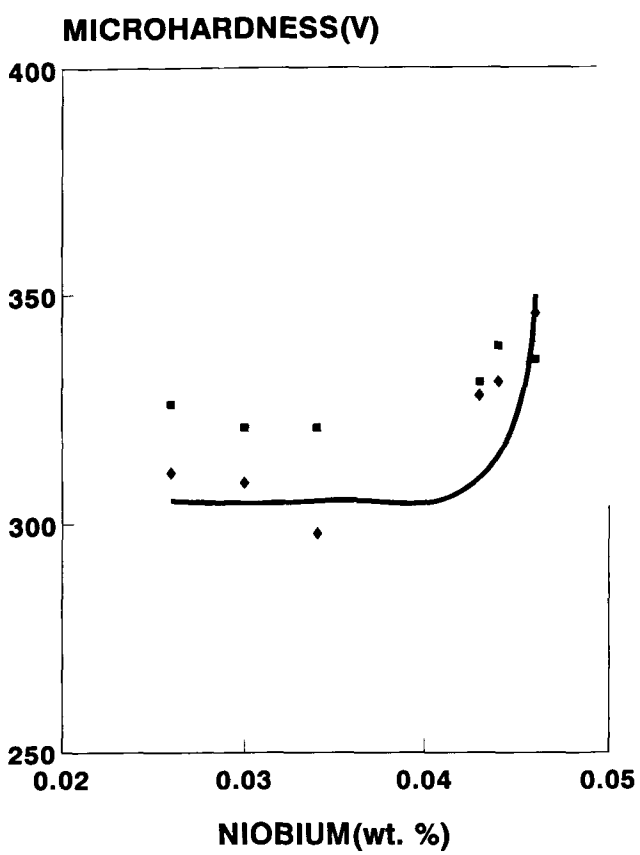

Fig. 9 Effect of niobium content on the microhardness of the ferrite phase after 10% (rhombuses) and 50% (squares) of cold deformation and aging for 0.5 h at 100 °C in boiling water

Acknowledgments

The present work was supported by DGAPA-UNAM grant IN300791. F. Estevez and C. Molina of SICARTSA provided steel and valuable statistical information. The technical support of J.L. Albarran, O. Flores, A. Gonzales, and R. Lima is gratefully acknowledged. L. Martinez acknowledges the support of the J.S. Guggenheim Foundation.

References

1. BS 4449: 1988—"British Standard Specification for Carbon Steel Bars for the Reinforcement of Concrete," Committee Reference ISM/9, BSI Publications, Milton Keynes, U.K., May 1988, p 1-13
2. Y. Maehara and T. Nagamichi, *Mater. Sci. Technol.*, Vol 7, 1991, p 915
3. R. Abushosha, R. Vipond, and B. Mintz, *Mater. Sci. Technol.*, Vol 7, 1991, p 1101
4. E. Valdez and C.M. Sellars, *Mater. Sci. Technol.*, Vol 7, 1991, p 622
5. H.J. Kestenbach, J.A. Rodrigues, and J.R. Dermonde, *Mater. Sci. Technol.*, Vol 5, 1989, p 29
6. Y. Maehara, K. Yasumoto, H. Tomono, T. Nagamichi, and Y. Ohmori, *Mater. Sci. Technol.*, Vol 6, 1990, p 793
7. T. Gladman et al., Effects of Second Phase Particles on the Mechanical Properties of Steel, The Iron and Steel Institute, London, 1971, p 68

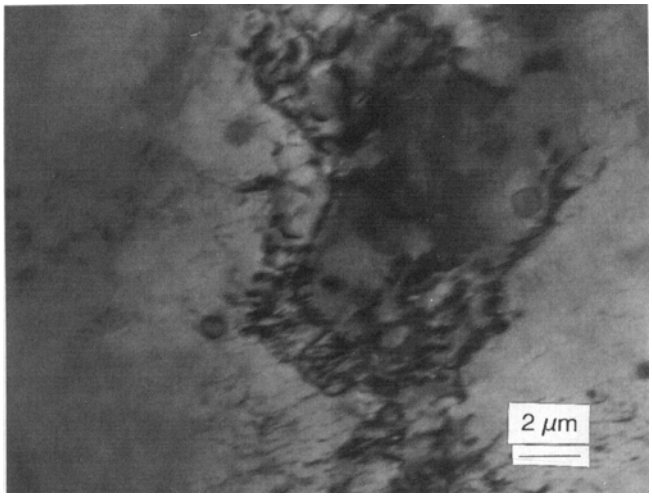

(a)

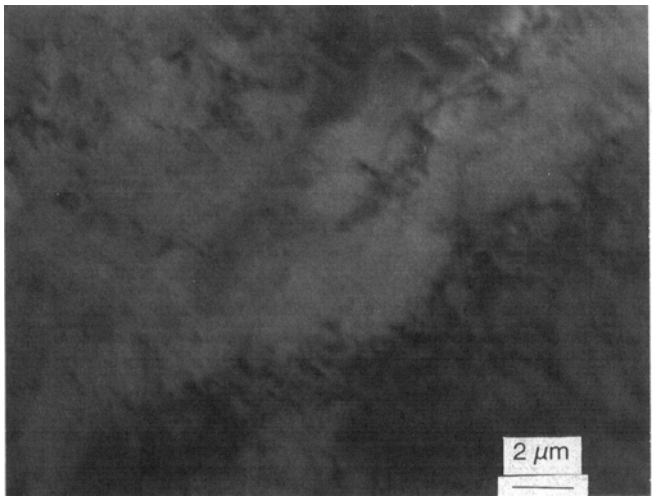

(b)

Fig. 10 TEM bright field image of sample 3 of Table 1 deformed 50%. (a) Dislocations around several large niobium-rich precipitates. (b) After aging. Very fine precipitates and few large precipitates. Source: Ref 17

8. I. Kozasu and J. Tanaka, *Sulphide Inclusions in Steels*, American Society for Metals, 1975, p 286
9. D.C. Hilty and W. Crafts, *Trans. AIME*, Vol 188, 1950, p 414
10. I. Kozasu and J. Tanaka, *Sulphide Inclusions in Steels*, American Society for Metals, 1975
11. I. Kozasu and H. Kubota, *Trans. Iron Steel Inst. Japan*, Vol 11, 1971, p 321
12. M. Korchynsky and H. Stuart, Low Alloy High Strength Steels, *Proc. London-Scandinavian Conf.*, Nuremburg, 1970, p 17
13. V. Castaño and L. Martínez, *J. Mater. Res.*, Vol 15 (No. 3), 1990, p 658
14. J.D. Baird, *Metall. Reviews*, No. 4, London, Iliffe, 1963
15. F.B. Pickering and T. Gladman, Special Report 81, Iron and Steel Institute, 1963, p 10
16. K. Hulka and F. Heisterkamp, *Steel India*, April 1985, p 1
17. B. Campillo et al. *J. Mater. Sci.*, Vol 27, 1992, p 1365-1368